Physica B 184 (1993) 470–480
North-Holland

PHYSICA B

Magneto-optical and magneto-transport studies of electron–electron interactions in organic conductors using fields up to 50 T

J. Singleton[a], F.L. Pratt[a], M. Doporto[a], J.M. Caulfield[a], S.O. Hill[a], T.J.B.M. Janssen[b], I. Deckers,[c] G. Pitsi[c], F. Herlach[c], W. Hayes[a], J.A.A.J. Perenboom,[b] M. Kurmoo[d] and P. Day[d]

[a]*Department of Physics, Clarendon Laboratory, University of Oxford, UK*
[b]*High Field Magnet Laboratory, University of Nijmegen, The Netherlands*
[c]*Laboratorium voor Lage Temperaturen en Hoge-Veldenfysica, Katholieke Universiteit, Leuven, Belgium*
[d]*Royal Institution, London, UK*

This paper reviews our recent studies of charge-transfer salts of the ion bis(ethylenedithio)tetrathiafulvalene (ET). The first part describes magneto-transport measurements which demonstrate modifications of the band structures of $(ET)_2KHg(SCN)_4$ and β''-$(ET)_2AuBr_2$ due to antiferromagnetic order; the antiferromagnetism is probably caused by the presence of spin-density waves. The second part reports cyclotron resonance studies of $(ET)_2KHg(SCN)_4$, $(ET)_2NH_4Hg(SCN)_4$ and $(ET)_2Cu(SCN)_2$, which reveal effective masses between $0.4m_e$ and $1.2m_e$. In contrast, magneto-transport measurements reveal masses between $2.0m_e$ and $3.5m_e$. The difference between the results is thought to indicate the strength of electron–electron interactions in these materials.

1. Introduction

Semiconductor heterostructures form just one example of the many ways in which physicists construct artificial structures to produce 'tailor-made' band-structure. Another approach is to use small organic molecules to build up solids with desirable (and eventually controllable) metallic, semiconducting or even superconducting properties [1]. Much of the current work in this field centers on charge-transfer salts, systems in which a number of molecules jointly donate an electron to another ion (the anion), thereby producing a stable crystalline lattice [2,3]. Within this family of compounds, charge-transfer salts of the ion bis(ethylenedithio)tetrathiafulvalene (BEDT–TTF or ET) [1–3] form a versatile system for the study of band formation; by varying the anion X in the salt $(ET)_nX$, the stoichiometry and band-filling may be adjusted, producing metallic, semimetallic, or semiconducting compounds. Indeed, the properties of ET salts encompass many of the disciplines of condensed matter physics; one member of this family provided us for a long time with the highest-temperature organic superconductor [2,3], whilst others combine antiferromagnetism with metallic conductivity [4–7]. The compounds are also of interest in the study of electron–electron interactions in narrow-bandwidth metallic systems, and have much in common with both high-T_c superconductors and heavy fermion compounds [3,8,9].

Figure 1 shows the crystal structure of β''-$(ET)_2AuBr_2$ and illustrates many of the typical structural properties of ET salts [2,3]. The ET molecules stack in two-dimensional (2D) planes, separated by layers of $AuBr_2$ anions. Transfer of electrons between ET molecules therefore occurs readily within the 2D planes, but much less

Correspondence to: J. Singleton, Department of Physics, Clarendon Laboratory, University of Oxford, Parks Road, Oxford OX1 3PU, UK.

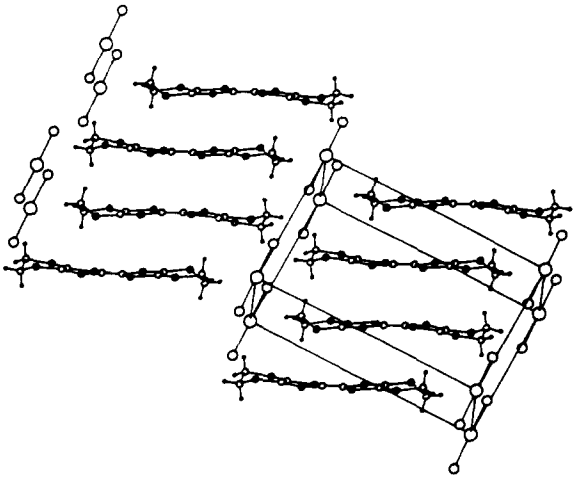

Fig. 1. Structure of β″-$(ET)_2AuBr_2$ showing the alternating layers of ET molecules and anions.

readily in the perpendicular direction through the anion layers. As a result, the band structures and electrical properties of ET salts are rather 2D. Figure 2 shows the Brillouin zone and Fermi surface [10] for $(ET)_2NH_4Hg(SCN)_4$ and for $(ET)_2KHg(SCN)_4$ calculated with an extended Hückel Model using their room temperature crystal structures, which are almost identical. As in many ET salts, the Fermi surface consists of a quasi 1D open section (electrons) and a closed 2D hole pocket. The weak inter-plane coupling causes a slight warping of the Fermi surface in the direction perpendicular to the 2D plane, i.e. the hole pocket in fig. 2 is a warped cylinder, rather than a true 2D Fermi line. ET salts with

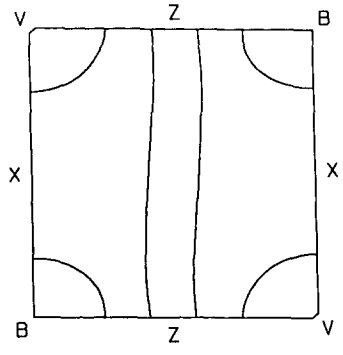

Fig. 2. Calculated Brillouin zone and Fermi surface of $(ET)_2KHg(SCN)_4$ and $(ET)_2NH_4Hg(SCN)_4$ (after ref. [10]).

smaller anions (i.e. thinner anion layers) are less 2D, and hence have more strongly warped Fermi surfaces; e.g., both neck and belly orbits around the hole Fermi cylinder have been observed as beating of the Shubnikov–De Haas oscillations (SDHO) in $(ET)_2I_3$ [11].

Altering the anion causes changes in the packing of the ET ions, enabling the molecular overlap and band-filling to be adjusted with sometimes dramatic results; e.g., the superconducting transition temperature T_c may be raised by a factor ~3 in the β-phase ET salts by changing the anion [2,3].

In the following sections we shall review some of our recent measurements on ET salts, emphasising results obtained using high magnetic fields. Whereas many ET salts have rather 'conventional' 2D metallic behaviour, we choose to concentrate here on ET salts or experiments which exhibit manifestations of carrier–carrier interactions, such as effective mass renormalisation, antiferromagnetism and superconductivity.

The samples used in our work are grown electrochemically [4]; the crystals are in general small ($\lesssim 1 \times 1 \times 0.1\,mm^3$) and black distorted diamond-shaped platelets, with the platelet plane defined by the highly conducting 2D directions. For magnetoresistance (MR) measurements gold wires are attached to both platelet faces using Pt paint. Standard AC current techniques (5–150 Hz) are used for all measurements except for pulsed field studies, where frequencies of 300 kHz or DC currents are employed. To avoid sample heating, currents are generally 0.2–20 μA. The crystals are studied in dilution refrigerators and ^{3}He and ^{4}He cryostats, some of which allow the sample to be rotated in-situ; magnetic fields are provided by superconductive, resistive, hybrid and pulsed magnets at Oxford, Nijmegen and Leuven. Further details are given in refs. [4,5].

2. Magnetoresistance (MR) measurements and the existence of antiferromagnetic order

Predominantly 1D substances such as the TMTSF charge-transfer salts have open (quasi-

1D) Fermi surfaces which are prone to spin-density wave (SDW) formation, due to their almost perfect nesting characteristics [2,3]. The SDW leads to antiferromagnetic behaviour and a band-gap at the Fermi energy which results in a metal–insulator transition. However, in spite of the presence of the quasi-1D band in ET salts (fig. 2) there was little evidence of SDW formation until recently. In this section, we shall describe MR data which show that SDWs can occur in ET salts [4–7,12], but that their effects are more subtle than in e.g. TMTSF salts, due to the presence of the 2D carriers.

2.1. $(ET)_2KHg(SCN)_4$

Some superconducting ET salts, such as $(ET)_2Cu(SCN)_2$, have a T_c above 10 K and have therefore attracted much interest [2,3]. Anion chemistry has shown that it is possible to improve T_c by enlarging the unit cell [2,3], and, following this idea, $(ET)_2KHg(SCN)_4$ and $(ET)_2NH_4Hg(SCN)_4$ were synthesised as modifications of $(ET)_2Cu(SCN)_2$ [2–4]. Figure 3 shows MR measurements on the former two salts, recorded using pulsed fields at Leuven [13]. $(ET)_2NH_4Hg(SCN)_4$, a superconductor with $T_c \simeq 1.15$ K, shows a series of SDHO growing in amplitude with increasing field in the manner predicted by the Lifshitz–Kosevich (LK) formula [4,14], and with a periodicity close to that expected from the area of the 2D hole pocket shown in fig. 2; i.e. 'conventional' behaviour. However, $(ET)_2KHg(SCN)_4$, which is metallic down to 100 mK [4,7], shows a large drop or 'kink' [15] in the MR at ~22 T, and then exhibits SDHO which grow strongly in amplitude. The different behaviour of the two salts, which have virtually identical crystal structures, excited great interest [15] and so a detailed study was undertaken [4].

Figure 4(a) shows the MR of two crystals of $(ET)_2KHg(SCN)_4$ at 0.5 K, measured with the field applied perpendicular to the (a,c) (2D) plane. Both samples exhibit an MR which rises to a peak before decreasing, and superimposed on this are SDHO. In each case there is hysteresis in the MR; that recorded with the field sweeping upwards is generally larger than that recorded on the downsweep. Note also that the size of the hysteresis is sample dependent.

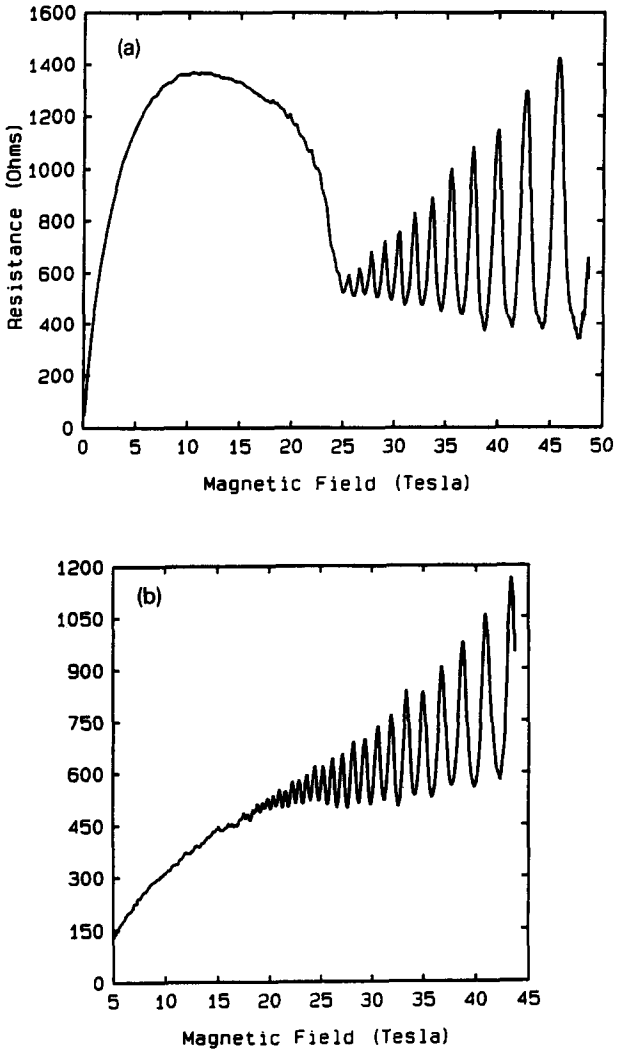

Fig. 3. Magnetoresistance of $(ET)_2KHg(SCN)_4$ (a: $T = 0.9$ K) and $(ET)_2NH_4Hg(SCN)_4$ (b: $T = 1.9$ K), measured using pulsed magnetic fields.

MR data from fig. 4(a) are plotted in fig. 4(b) with the slowly varying background subtracted. Two primary SDHO frequencies are present in both samples causing beating; one of the SDHO frequencies, $B_{F1} = 670 \pm 5$ T, is present in all samples studied, but the other frequency B_{F2} is sample or cooling-method dependent, and ranges from $\sim B_{F1} + 50$ T to $\sim B_{F1} + 200$ T. In

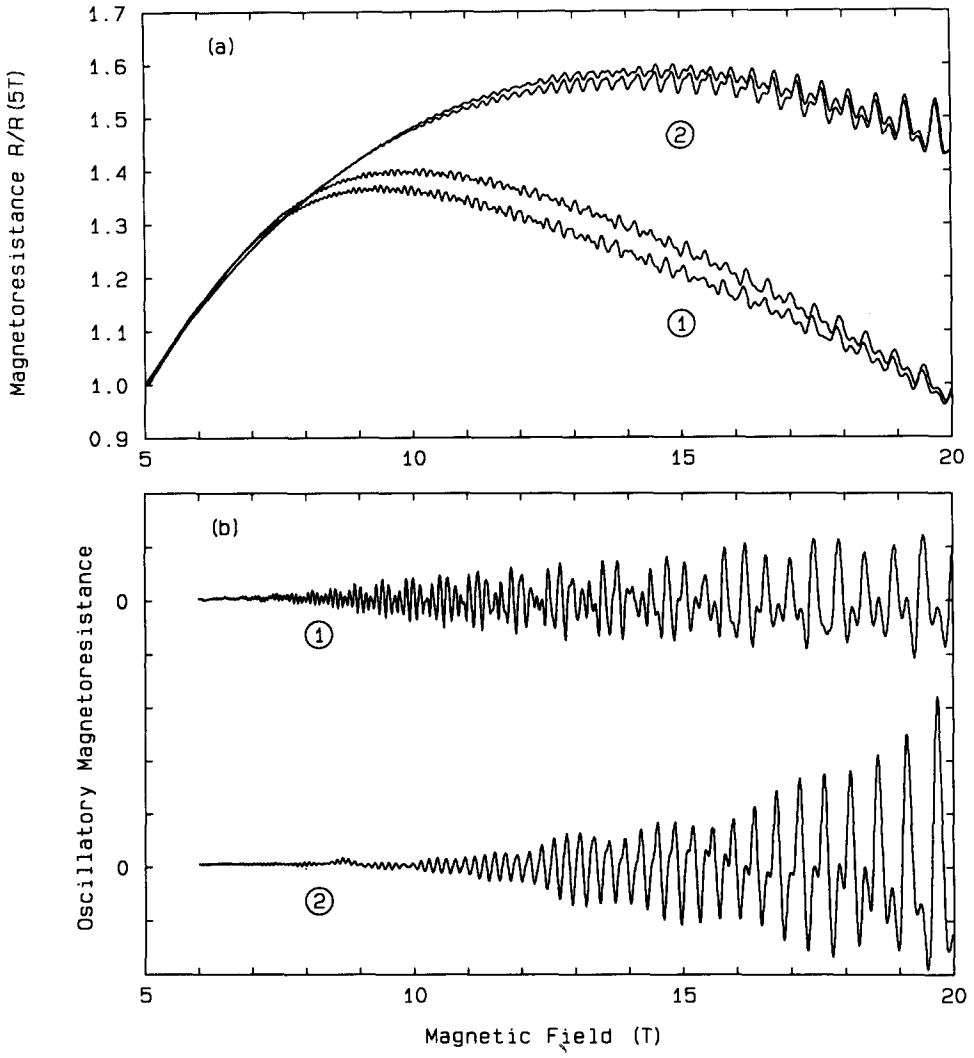

Fig. 4. MR of two $(ET)_2KHg(SCN)_4$ crystals (1 and 2). Raw data for upsweeps and downsweeps of the field. SDHO with the background MR removed.

fig. 4 sample 1 has $B_{F2} \simeq 860$ T, whereas sample 2 has $B_{F2} = 790$ T, leading to the different beat periodicities seen in the SDHO. Note also (fig. 4(a)) that the degree of MR hysteresis correlates with the size of the frequency difference between B_{F1} and B_{F2}, and that this appears true for all samples studied [4].

Figure 5(a) shows the high-field MR for several angles θ between the field and the sample surface normal. For $\theta \lesssim 50°$, a large drop or 'kink' [4–7,15] in the resistance occurs at ~22 T (see also fig. 3); at higher fields only one series of SDHO is observed, with a frequency $B_F = 656 \pm 10$ T ($= B_{F1}$ to within experimental errors) and the hysteresis almost vanishes. As θ increases, the 'kink' transition gradually moves to a lower total field with the approximate functional form $B = B_0 \cos^{1/2}\theta$ (see fig. 6(b)), until it vanishes at $\theta \simeq 57°$. Meanwhile, the high-field (>23 T) SDHO frequency follows the $1/\cos\theta$ dependence expected of a 2D metal, and there are the amplitude and harmonic content oscilla-

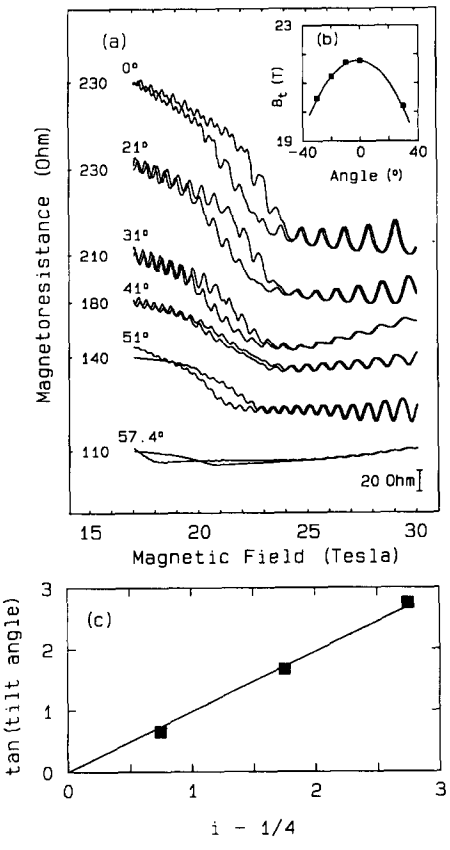

Fig. 5. (a) High-field MR showing a drop ('kink') in resistance around 22 T; the traces are offset for clarity (T = 490 mK). (b) The angular dependence of the 'kink' (points) fitted to a $\cos^{1/2}\theta$ dependence (line). (c) Plot of tan θ_y versus $i - \frac{1}{4}$. Data are points; the solid line is a fit (see text).

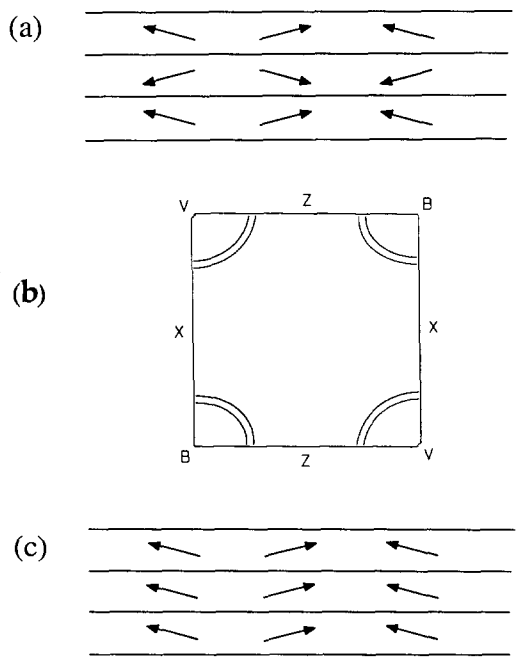

Fig. 6. (a) Proposed canted arrangement of dipoles in the SDW state of $(ET)_2KHg(SCN)_4$. (b) Resultant Fermi surface. (c) Dipole arrangement at fields above the 'kink' transition.

tions expected from the varying spin to cyclotron splitting ratio as θ increases. Figure 5(a) also illustrates that there are oscillations in the background MR. The background MR between 23 and 30 T exhibits maxima at angles 33 ± 1°, 59 ± 1° and 70 ± 1°. This is a common phenomenon in ET salts, and has been explained by Yamaji [16], who showed that at certain angles all the semiclassical k-space closed orbits around the warped cylindrical Fermi-surface have approximately the same area. This means that the density of states at the Fermi energy is greatly enhanced, resulting in a maximum in the background MR. The angles θ_y at which this occurs are given by $bk_F \cos\theta_y = \pi(i - \frac{1}{4})$ where b is the inter-plane spacing, k_F is the mean radius of the Fermi surface and i is an integer. Figure 5(c) shows the experimental values of $\cos\theta_y$ versus i; the data lie on a straight line, of gradient π/bk_F. Taking $k_F = (4\pi eB_F/h)^{1/2}$ with $B_F = 656$ T we find b = 2.1 ± 0.1 nm, close to the value b = 2.0 nm obtained from X-ray crystallography measurements [4,10].

It therefore appears that the MR behaviour above the transition is 'conventional'. Indeed, if we compare the predicted area of the 2D hole pocket (fig. 3(c)) with the SDHO frequency ($B_F = 656 \pm 10$ T) the agreement is very good. Therefore, above the 22 T transition the experimental MR is in agreement with the band structure calculation, whereas the situation is rather more complicated at lower fields.

The susceptibility measurements show that $(ET)_2KHg(SCN)_4$ is antiferromagnetic below ~8 K, probably due to an incommensurate SDW associated with the quasi-1D band [17]. A SDW would open up an energy gap along the quasi-1D

band, preventing the electrons taking part in the electrical conductivity; this is supported by the very isotropic MR below 22 T [4]. The remaining carriers (in the 2D pockets) and the SDW will form an interacting system, as suggested by the changes in MR occurring at the same temperature as the onset of antiferromagnetism [4–7,17]. In order to explain the presence of the 'kink' transition and the behaviour above and below it we suggest that, at low fields, the system is not only antiferromagnetically ordered within the plane, but that there is also a magnetic superlattice in the b^* direction (perpendicular to the 2D plane), causing a doubling of the unit cell along this axis. A possible mechanism for this is canted antiferromagnetic order within each plane, with the canting direction alternating from one layer to another (fig. 6(a)). If the spin distribution acts as a static background from which the conduction electrons scatter, the band-structure will be divided into two magnetic subbands separated by a band-gap [4]. The formation of a magnetic band-gap will double the number of SDHO frequencies; a schematic representation of the possible Fermi surface is shown in fig. 6(b). High external magnetic fields may change the magnetisation so that all planes become equivalent (fig. 6(c)), hence removing the magnetic band-gap; a mechanism suggested by magnetization data [7] is for the canting direction to become uniform in all planes. The number of states available for small-k scattering at the Fermi surface will be lowered (cf. figs. 6(b) and 2), thus reducing the resistance. We therefore identify this change in magnetic order with the 'kink' transition occurring at ~22 T. (Note also that typical magnetic energies (cyclotron- or spin-splitting) at 22 T are of a similar size to the inter-plane energy suggested by the transition temperature of ~8 K [4,5].) The varying degree of internal magnetic order between samples will lead to different splittings between B_{F1} and B_{F2}, and the hysteresis in MR will occur because on the downsweep, the spin system will be more ordered, leading to less spin-disorder scattering [4]; lower resistances are almost invariably seen on the downsweep.

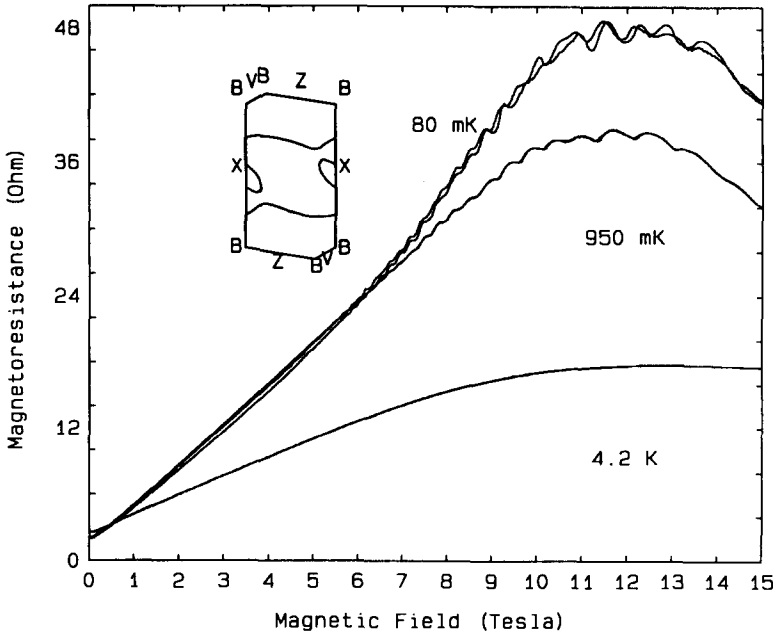

Fig. 7. MR of β″-$(ET)_2AuBr_2$ for various temperatures; upsweeps and downsweeps are shown. The inset shows the calculated Brillouin zone and Fermi surface.

2.2. β''-$(ET)_2AuBr_2$

Figure 7 shows MR data from β''-$(ET)_2AuBr_2$ for both up- and downsweeps of the field, which is applied perpendicular to the (a,c) (i.e. 2D) plane [12]. A prominent series of SDHO can be seen at 80 mK and 950 mK, apparently modulated by other frequencies. There is also hysteresis between the upsweep and downsweep data at 80 mK, indicating the presence of an internal magnetic field. Fourier transforms of the MR show peaks due to two SDHO series, B_{Fi} = 180 T and B_{Fii} = 39 T, along with the sums and differences of these two primary frequencies and their harmonics [12]. Hence, series B_{Fi} and B_{Fii} correspond to closed pockets ~2.5% and ~0.5% of the room temperature Brillouin zone (RTBZ) area [12]. The calculated Fermi surface [12] (fig. 7) has just one closed hole pocket of ~5% of the RTBZ area, together with a pair of open sections. Although the closed hole pocket is at first sight a factor of two too large to correspond to SDHO series B_{Fi}, it should be remembered that the curvature of the band containing the closed pocket is large, so that small adjustments of e.g. the overlaps could result in a large reduction in pocket area. However, the calculated Fermi surface contains no obvious candidate for series B_{Fii}. We therefore propose that the additional SDHO frequencies are the result of closed pockets produced by a Zc SDW modulation driven by the nesting properties of the quasi-1D part of the Fermi surface. Evidence for this SDW has been seen in the spin susceptibility below ~20 K [12]. The result of the SDW modulation is seen in fig. 8 (inset); a small pocket (hole-like) is produced close to V, along with a very anisotropic closed section of Fermi surface (electron-like); the latter is orientated in the correct sense to be responsible for the MR anisotropy observed in this material [12]. The band-filling is such that there should be equal numbers of electrons and holes, so that the total area of the two hole pockets should be the same as the area of the electron pocket. In this way, if we identify the two hole pockets with SDHO series B_{Fi} and B_{Fii}, the SDHO due to the electron pocket should occur at the sum of these frequencies, and such a peak is indeed present [12].

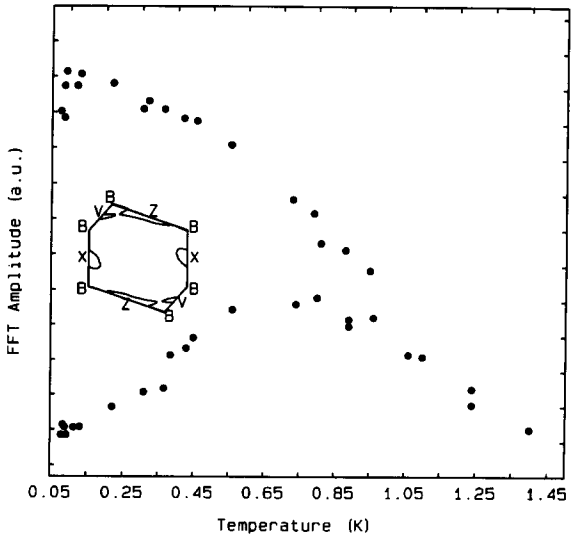

Fig. 8. Fourier amplitude of the dominant SDHO series (~180 T) in β''-$(ET)_2AuBr_2$ versus temperature. Amplitudes for downsweeps of the field are lower than those for upsweeps below ~0.9 K. The inset shows the modified Brillouin zone and Fermi surface due to the SDW.

Although the presence of the SDW accounts successfully for the observed SDHO frequencies, details of the low-temperature phase diagram remain to be resolved, as indicated in fig. 8, which shows the Fourier amplitude of the B_{Fi} series of SDHO for both upsweeps and downsweeps of the field. Below ~0.9 K the latter are much lower than the former, but above this temperature the two are indistinguishable. In addition, the resistance at fields ~15 T has an activated character above ~0.9 K, but not below [13]. This temperature (~0.9 K) therefore appears to represent an additional phase boundary within the SDW phase, and further investigations are under way [13].

3. Magneto-optical studies

The effective mass is an important parameter in studies of superconductors, as it is a measure of the density of states at the Fermi level, which in turn determines the electron–phonon coupling strength [2,3]. Some time ago it was noted that

there is a large enhancement of the effective mass m_F measured using the temperature dependence of the SDHO (or De Haas–Van Alphen oscillations) over the predicted band mass in the 10.4 K superconductor $(ET)_2Cu(SCN)_2$ [8]. In addition, Toyota et al. [9] pointed out that band-structure calculations in ET salts almost always reproduce the experimentally observed Fermi surface shapes fairly reliably, but overestimate the bandwidth (i.e. underestimate the effective mass). Toyota et al. [9] plotted experimental values of m_F against the Dingle temperature T_D ($\propto 1/\tau$, where τ is the scattering time) for several superconducting ET salts and noted that the materials with $T_c > 7$ K fell into the high-m_F ($>2m_e$), low-T_D (long-τ) quadrant of the plot, whereas metals and superconductors with $T_c <$ 4 K had smaller m_F ($<m_e$) and larger T_D; nevertheless all of the materials had similar resistivities and scattering *lengths*. These results were explained by introducing many-body effects [8,9]. The resultant electron self-energy leads to a renormalisation of *both* m_F and τ by the same parameter Z, leaving the resistivity and the scattering length unchanged. Assuming that the 'poor' superconductors have unrenormalised masses, Toyota et al. postulated that $Z \simeq 10$ [9], but in the absence of further data were unable to state whether this was due to electron–phonon or electron–electron interactions, or both.

Cyclotron resonance (CR) measurements have an important role to play in such studies since, according to Kohn's theorem [18], the effective mass m_{CR} measured by CR is independent of electron–electron interactions, giving the band mass renormalised only by electron–phonon interactions, whereas m_F, the mass measured e.g. by SDHO, will additionally be influenced by the electron–electron interactions. In the language of interacting Fermi liquid theory the ratio of the two masses, m_F/m_{CR}, is equal to $(1 + F_1^s/3)$, where F_1^s is the parameter which characterises quasiparticle interactions [19]. Thus, an experimental comparison of m_F and m_{CR} gives a direct gauge of the strength of electron–electron interactions. In the remaining part of this paper, we shall describe the first cyclotron resonance measurements carried out on ET salts.

3.1. *Cyclotron resonance of $(ET)_2KHg(SCN)_4$, $(ET)_2NH_4Hg(SCN)_4$ and $(ET)_2Cu(SCN)_2$*

For CR measurements the crystals are arranged in the form of a mosaic with the highly conducting planes perpendicular to the magnetic field. The far-infrared (FIR) laser system used as light source has been described in detail elsewhere [20]. Carbon bolometers are used to measure the incident, transmitted and reflected radiation, and the reflected and transmitted signals normalised to the incident signal. Magnetic fields are provided by a 17 T superconductive solenoid or a 20 T Bitter magnet.

The measured FIR magneto-reflectivity of $(ET)_2KHg(SCN)_4$ at 1.2 K is shown in fig. 9 for

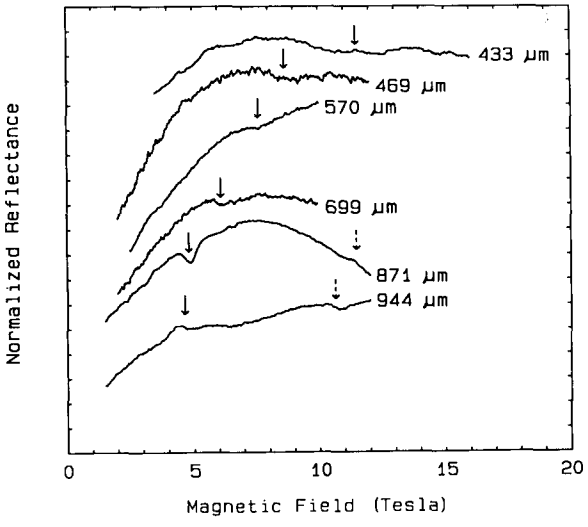

Fig. 9. Normalized magneto-reflectance of $(ET)_2KHg(SCN)_4$ at 1.2 K for different radiation energies. The cyclotron resonance features are marked with arrows.

Table 1
Experimental values of T_c, m_F (±3%) and m_{CR} ($\pm 0.02m_e$) for the ET salts studied. Two values of the masses are given for $(ET)_2KHg(SCN)_4$, as two series of SDHO and two CR are present.

Salt	T_c	m_F	m_{CR}
$(ET)_2Cu(SCN)_2$	10.4 K	$3.5m_e$	$1.18m_e$
$(ET)_2NH_4Hg(SCN)_4$	1.1 K	$2.5m_e$	$1.17m_e$
$(ET)_2KHg(SCN)_4$	metallic	$2.0m_e$	$0.40m_e$
		$2.4m_e$	$0.94m_e$

several laser wavelengths [5]. Two sharp features are observed occurring at fields which are proportional to the FIR energy, the characteristic behaviour of CR; as we saw above, the 2D section of the Fermi surface of this material is divided into two pockets by the magnetic interactions [4,5], and so two CR are expected. The resonances are superimposed on the gently varying background magnetoreflectance and instrumental response. The strongest of the two features appears as a dip in reflectivity at 5 T with 871 μm radiation, and as such is very similar in form to CR reflectivity signals seen from 2D electron gases in semiconductor heterostructures when the underlying reflectivity of the structure is high [20]. In contrast to the ~10% modulation of the reflectivity seen in the latter systems, however, the $(ET)_2KHg(SCN)_4$ small skin-depth means that the CR leads to only a ~0.6% change in reflectivity. At higher energies the dip becomes wider and shallower, whereas for longer wavelengths the CR is observed as a peak. The latter behaviour is also seen in heterostructures under conditions of changing background reflectance [20]. The sharp change in behaviour between 871 μm and 944 μm may be due to a low energy lattice phonon. The cause of the broadening of the CR at higher energies is unknown; it may represent the onset of a resonant coupling to a phonon mode (cf. ref. [20]). The weaker CR at higher fields (fig. 1) also exhibits changes in shape as a function of wavelength. The field positions of both CR features are plotted against energy in [5]. Effective masses of $m^*_{CR1} = (0.40 \pm 0.02)m_e$ and $m^*_{CR2} = (0.94 \pm 0.02)m_e$ are estimated from the linear slopes of the plots of radiation energy against CR field position.

$(ET)_2NH_4Hg(SCN)_4$ and $(ET)_2Cu(SCN)_2$ have single 2D closed hole pockets in their Fermi surfaces (see e.g. fig. 2 and refs. [2,3]), and so only a single CR is expected. Figure 10 shows transmission through an $(ET)_2Cu(SCN)_2$ crystal array of laser light of wavelength 1223 μm (1.02 meV) as a function of magnetic field. Two prominent features are observed; at low fields the superconducting–normal transition is seen as a region of increasing transmission, whilst at

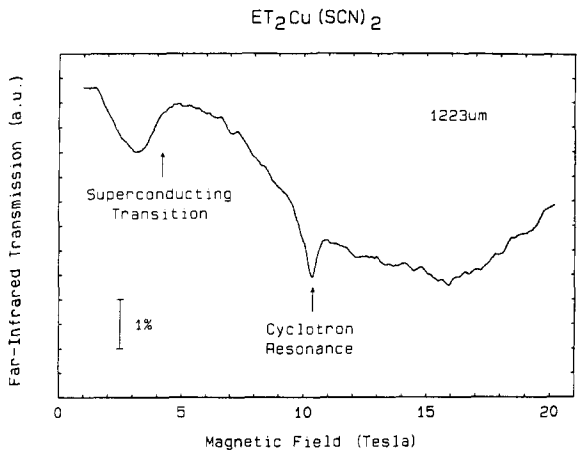

Fig. 10. Transmission through an array of $(ET)_2Cu(SCN)_2$ crystals of laser light of wavelength 1223 μm (1.02 meV) as a function of magnetic field ($T = 1.2$ K).

higher fields the single CR is observed as a sharp dip [21]. Similar results were obtained by using several other FIR wavelengths. $(ET)_2NH_4Hg(SCN)_4$ crystals also exhibited a single CR of similar size, but no superconducting–normal transition; the experiments were carried out at 1.2 K, above T_c.

In order to evaluate m_F for the ET salts studied using CR, the amplitudes of the SDHO were measured as a function of temperature between 0.5 K and 5 K and fitted using the LK formula [13,14,22]. Great care must be taken in this procedure in order to avoid misleading results; in our work m_F is the only adjustable parameter, and B_F and T_D are found separately by a direct fit to ten periods of SDH oscillations between 15 and 20 T using the LK formula [13,22]. Particular attention is paid to uncertainties of parameters in the fitting procedure [22]. Care must also be taken when using pulsed fields, where sample heating often leads to underestimates of the effective mass [13]. Experimental values of m_F and m_{CR} are shown in the table.

The data in the table show that CR experiments, which are insensitive to electron–electron interactions, reveal smaller masses in ET salts than those deduced from SDHO measurements. In addition, the CR results indicate bandwidths which are similar to, or wider than, the calcu-

lated values. As electron–phonon interactions are expected to renormalise *both* m_{CR} and m_F equivalently [5], the experiments reported here indicate that the major part of the observed difference between calculated bandwidths and those measured using SDHO is due to electron–electron interactions, which lead to an enhancement of ~2–5 in the effective mass of the 2D holes.

The electron–electron interaction responsible for the effective mass renormalisation can be described by a Hubbard model with an effective on-site Coulomb correlation energy U_{eff}. Mass renormalisation in the Hubbard model has been considered by Brinkman and Rice [23] using the Gutzwiller approximation. For a half-filled band the renormalisation factor is $(1-(U_{eff}/8\varepsilon)^2)^{-1}$ where ε is the average energy of the electrons. For the present purposes a simplified view of the band structure of ET salts [2,5,10] will be taken. A dimer is regarded as the basic unit, which produced two dimer bands, the upper band being half-filled. The measured mass enhancements of ~2–5 imply that $U_{eff}/8\varepsilon$ is between 0.7 and 0.9. The average energy of electrons in the upper subband is estimated to be ~60 meV from the band-structure [5,10]. This leads to a value for U_{eff} for the dimer in the range 0.4–0.5 eV; in this model U_{eff} is associated with the intra-dimer correlation energy V_D and the values obtained here are entirely consistent with typical values for V derived from optical spectra of a wide range of charge transfer salts [24].

In summary, we have measured CR in ET salts for the first time; the results indicate low carrier effective masses between $0.4m_e$ and $1.2m_e$. In contrast, SDHO measurements reveal higher masses between $2.0m_e$ and $3.5m_e$. We believe that the difference between the transport and cyclotron masses is an indication of the strength of electron–electron interactions in the materials.

4. Concluding remarks

This paper has reviewed some of the physics which can be done with ET salts in high magnetic fields. During the paper, many similarities between the ET salts and high-T_c superconductors may have become apparent [2,3], e.g.: 2D band structures with closed Fermi surfaces and weak inter-plane coupling; low carrier (hole) densities ($\sim 10^{21}\,cm^{-3}$), implying less screening, leading to the importance of electron–electron interactions; competition between antiferromagnetism and superconductivity; heavy effective masses (~ 2–$5m_e$) leading to small Fermi velocities ($\sim 10^5\,m\,s^{-1}$) and also Fermi energies (~0.1 eV). Many of these properties are also shared with heavy-fermion systems. The attraction of ET salts is that they contain all of this interesting physics but may be studied using reasonable laboratory fields (10–15 T) and temperatures (0.08–5 K). They may, therefore, well be the first systems on which theoretical approaches to high-T_c superconductors or heavy-fermion systems are tested.

Acknowledgements

This work is supported by the Science and Engineering Research Council (UK). The Nijmegen Laboratory is supported by the Stichting voor Fundamenteel Onderzoek der Materie (FOM) and by the European Community Large Installations Plan. The pulsed field work at Leuven was carried out by J.C. under the ERASMUS scheme. J.S. would like to thank the KU Leuven for a visiting professorship, which greatly assisted the preparation of the material in this paper.

References

[1] For a review, see, e.g., Synth. Met. 41–43 (1991).
[2] T. Ishiguro and K. Yamaji, Organic Superconductors (Springer-Verlag, Berlin, 1990).
[3] V.Z. Kresin and W.A. Little (eds.), Organic Superconductivity (Plenum Press, New York, 1990).
[4] F.L. Pratt, J. Singleton, M. Doporto, A.J. Fisher, T.J.B.M. Janssen, J.A.A.J. Perenboom, M. Kurmoo, W. Hayes and P. Day, Phys. Rev. B 45 (1992) 13 904.
[5] J. Singleton, F.L. Pratt, M. Doporto, W. Hayes, T.J.B.M. Janssen, J.A.A.J. Perenboom, M. Kurmoo and P. Day, Phys. Rev. Lett. 68 (1992) 2500.

[6] T. Sasaki and N. Toyota, Solid State Commun. 82 (1992) 447.
[7] J.S. Brooks, C.C. Agosta, S.J. Klepper, M. Tokumoto, N. Kinoshita, H. Anzai, S. Uji, H. Aoki, A.S. Perel, G.J. Athas and D.A. Howe, Phys. Rev. Lett. 69 (1992) 156.
[8] F.L. Pratt, J. Singleton, M. Kurmoo, S.J.R.M. Spermon, W. Hayes and P. Day, in: The Physics and Chemistry of Organic Superconductors, eds. G. Saito and S. Kagoshima, Springer Proceedings in Physics 51 (1990) 200.
[9] N. Toyota, E.W. Fenton, T. Sasaki and M. Tachiki, Solid State Commun. 72 (1989) 859.
[10] H. Mori, S. Tanaka, M. Oshima, G. Saito, T. Mori, Y. Maruyama and H. Inokuchi, Bull. Chem. Soc. Jpn. 63 (1990) 2183.
[11] W. Kang, G. Montambaux, J.R. Cooper, D. Jerome, P. Batail and C. Lenoir, Phys. Rev. Lett. 62 (1989) 2559.
[12] F.L. Pratt, M. Doporto, J. Singelton, T.J.B.M. Janssen, J.A.A.J. Perenboom, M. Kurmoo, W. Hayes and P. Day, Physica B 177 (1992) 333.
[13] J. Singleton, F.L. Pratt, M. Doporto, J. Caulfield, W. Hayes, I. Deckers, G. Pitsi, F. Herlach, T.J.B.M. Janssen, J.A.A.J. Perenboom, M. Kurmoo and P. Day, in: Proc. Int. Conf. on Science and Technology of Synthetic Metals, Göteborg, Sweden, August 12–18, 1992, to be published in Synth. Met.; M. Doporto, J. Caulfield, F.L. Pratt, J. Singleton, S. Hill, W. Hayes, J.A.A.J. Perenboom, M. Kurmoo and P. Day, ibid.
[14] D. Schoenberg, Magnetic Oscillations in Metals (Cambridge University Press, 1984).
[15] T. Osada, R. Yagi, A. Kawasumi, S. Kagoshima, N. Miura, M. Oshima, H. Mori, T. Nakamura and G. Saito, Synth. Met. 42 (1991) 2171; T. Osada, R. Yagi, S. Kagoshima, N. Miura, M. Oshima and G. Saito, Phys. Rev. B 41 (1990) 5428; Solid State Commun. 75 (1990) 901; M. Tokumoto, A.G. Swanson, J.S. Brooks, C.C. Agosta, S.T. Hannahs, N. Kinoshita, H. Anzai and J.R. Anderson, J. Phys. Soc. Jpn. 59 (1990) 2324.
[16] K. Yamaji, J. Phys. Soc. Jpn. 58 (1989) 1520.
[17] T. Sasaki, N. Toyota, M. Tokumoto, N. Kinoshita and H. Anzai, Solid State Commun. 75 (1990) 93, 97.
[18] W. Kohn, Phys. Rev. 123 (1961) 1242.
[19] K.F. Quader, K.S. Bedell and G.E. Brown, Phys. Rev. B 36 (1987) 156.
[20] C.J.G.M. Langerak, J. Singleton, J.A.A.J. Perenboom, F.M. Peeters, J.T. Devreese, D.J. Barnes, R.J. Nicholas, S. Huant, J.J. Harris, C.T. Foxon and B. Etienne, Phys. Scripta T39 (1991) 308.
[21] S. Hill, J. Singleton, F.L. Pratt, M. Doporto, W. Hayes, T.J.B.M. Janssen, J.A.A.J. Perenboom, M. Kurmoo and P. Day, in: Proc. Int. Conf. on Science and Technology of Synthetic Metals, Göteborg, Sweden, August 12–18, 1992, to be published in Synth. Met.; J. Singleton, F.L. Pratt, M. Doporto, J. Caulfield, W. Hayes, I. Deckers, G. Pitsi, F. Herlach, T.J.B.M. Janssen, J.A.A.J. Perenboom, M. Kurmoo and P. Day, ibid.
[22] M. Doporto, F.L. Pratt, J. Singleton, M. Kurmoo and W. Hayes, Phys. Rev. Lett. 69 (1992) 991.
[23] W.F. Brinkman and T.M. Rice, Phys. Rev. B 2 (1970) 4302.
[24] S. Mazumdar and S.N. Dixit, Phys. Rev. B 34 (1986) 3683.